

# K-Matrix Analysis of the ( $IJ^{PC} = 00^{++}$ ) Amplitude in the Mass Region up to 1550 MeV.

V.V.Anisovich and A.V.Sarantsev  
Petersburg Nuclear Physics Institute  
Gatchina, St.Petersburg 188350, Russia  
e-mail:anisovic@lnpi.spb.su  
vsv@hep486.pnpi.spb.ru

## Abstract

K-matrix analysis of the  $00^{++}$  wave is performed in the channels  $\pi\pi$ ,  $K\bar{K}$ ,  $\eta\eta$  and  $4\pi$  in the mass region up to 1550 MeV. The fit is based on the following data:  $p\bar{p}$  (*at rest*)  $\rightarrow \pi^0\pi^0\pi^0$ ,  $\pi^0\pi^0\eta$ ,  $\pi^0\eta\eta$  [1, 2],  $\pi N \rightarrow \pi\pi N$  [3, 4],  $\pi N \rightarrow K\bar{K}N$  [5] and the inelastic cross section of the  $\pi\pi$  interaction [6]. Simultaneous analysis of these data confirms the existence of the scalar resonances:  $f_0(980)$ ,  $f_0(1300)$  and  $f_0(1500)$ , the poles of the amplitude being at the following complex masses (in MeV):  $(1008 \pm 10) - i(43 \pm 5)$ ,  $(1290 \pm 25) - i(120 \pm 15)$ , and  $(1497 \pm 6) - i(61 \pm 5)$ . The fourth pole has sunk deeply into the complex plane:  $(1430 \pm 150) - i(600 \pm 100)$ . Positions of the K-matrix poles (which are referred to the masses of bare states) are at  $750 \pm 120$  MeV,  $1240 \pm 30$  MeV,  $1280 \pm 30$  MeV and  $1615 \pm 40$  MeV. Coupling constants of the K-matrix poles to the  $\pi\pi$ ,  $\eta\eta$  and  $K\bar{K}$  channels are found that allow us to analyze the quark and gluonic content of bare states. It is shown that  $f_0^{bare}(1240)$  and  $f_0^{bare}(1615)$  (which are strongly related to  $f_0(1500)$ ) can be considered as good candidates for scalar glueball.

Identification of scalar resonances in the mass region 800–2000 MeV and their classification in the  $q\bar{q}$ -nonets is the necessary step in a search for the lowest scalar glueball. The couplings of these states to the pseudoscalar mesons ( $\pi\pi$ ,  $K\bar{K}$ ,  $\eta\eta$ ,  $\eta\eta'$ ,  $\eta'\eta'$ ) are the glueball signature: the gluonic nature of the resonance reveals itself in the relations for branching ratios into these channels [7, 8].

Glueball spectra obtained in the QCD-inspired models [9, 10] as well as in the framework of the lattice QCD calculations [11, 12] are backing the expectation that the lowest scalar glueball is located in the mass region 1000–2000 MeV. However, the predictions for glueball mass can not be taken literally. The present lattice QCD calculations of glueball mass do not take into account quark degrees of freedom properly, while according to the rules of the  $1/N$ -expansion [13] the glueball can mix with  $q\bar{q}$ -components without suppression. A mass shift of the order of 100–300 MeV can easily be caused by an admixture of  $q\bar{q}$ -components.

Scalar resonances in the region 1000–1500 MeV have been investigated in a number of papers [1, 4, 14, 15] where it was shown that the data in this mass region can be described by the three scalar resonances:  $f_0(980)$ ,  $f_0(1300)$  and  $f_0(1500)$ . However, in these papers the K-matrix formalism has been used for the energy region below 1200 MeV, and the resonances  $f_0(1300)$  and  $f_0(1500)$  have been studied in the framework of the T-matrix technique. The T-matrix technique which is very effective in the determination of the poles of the physical amplitude cannot be applied to define the initial "bare" poles (related to the quark-antiquark or gluon-gluon interactions) because of resonances overlapping. The proper method to investigate the structure of the "bare" states is the K-matrix approach or the dispersion relation  $N/D$ -method, as was repeatedly emphasized in recent times (see, for example, ref. [16]).

In ref. [17] the resonance  $f_0(980)$  have been analyzed in the framework of a two-channel ( $\pi\pi$  and  $K\bar{K}$ ) K-matrix formalism. The expansion of the K-matrix analysis into the region of higher mass requires accounting for other open channels, namely,  $\eta\eta$  and  $4\pi$ . In the present paper we perform the four-channel K-matrix analysis of the following experimental data: meson spectra in the reactions  $p\bar{p}$  (*at rest*)  $\rightarrow \pi^0\pi^0\pi^0$ ,  $\eta\pi^0\pi^0$ ,  $\eta\eta\pi^0$  obtained by Crystal Barrel collaboration [1, 2], two-pion spectra in the reactions  $\pi^-p \rightarrow \pi^-\pi^+n$  (CERN-Münich collaboration [3]) and  $\pi^-p \rightarrow \pi^0\pi^0n$  (GAMS [4]), partial cross section  $\pi\pi \rightarrow K\bar{K}$  in the  $00^{++}$ -wave [5] and the inelastic cross section for the  $\pi\pi$  interaction [6]; the channels  $\pi\pi$ ,  $K\bar{K}$ ,  $\eta\eta$  and  $4\pi$  are taken into account.

Our analysis confirms the existence of three scalar resonances  $f_0(980)$ ,  $f_0(1300)$  and  $f_0(1500)$ ; the fourth pole of the scattering amplitude may correspond to a broad resonance at 1300–1600 MeV,  $f_0(1300/1600)$ . But the K-matrix solution is not unique. We have found two sets of solutions which describe well the data and give approximately the same positions for the poles of the physical amplitude and for the K-matrix poles. Coupling constants of the K-matrix poles to  $\pi\pi$ ,  $K\bar{K}$  and  $\eta\eta$  also coincide reasonably. But the solutions differ in the K-matrix background terms.

In the leading terms of the  $1/N$  expansion, quark combinatorics predict definite ratios for coupling constants of  $q\bar{q}$  mesons decaying into two pseudoscalar mesons: these ratios depend on the flavour content of the decaying meson. Based on this, we show that the

only lowest bare state has large  $s\bar{s}$  component, approximately the same as in the  $\eta$ -meson. The others have a small admixture of  $s\bar{s}$ . Two of them,  $f_0^{bare}(1240)$  and  $f_0^{bare}(1615)$ , are good candidates for a glueball: their coupling constants  $f_0^{bare} \rightarrow \pi\pi, K\bar{K}, \eta\eta$  coincide with predictions for the glueball decay.

**1) K-matrix technique.** We use standard K-matrix technique for the description of the meson scattering amplitudes in the  $00^{++}$ -state:

$$\hat{A} = \hat{K}(\hat{I} - i\hat{\rho}\hat{K})^{-1}, \quad (1)$$

where  $K_{ab}$  is a  $4 \times 4$  matrix ( $a, b=1,2,3,4$ ) with the following notations for meson states:  $1=\pi\pi$ ,  $2=K\bar{K}$ ,  $3=\eta\eta$  and  $4=\pi\pi\pi\pi$ . The phase space matrix is a diagonal one:

$$\rho_{ab} = \delta_{ab}\rho_a, \quad \rho_a = \sqrt{1 - \frac{4m_a^2}{s}}, \quad \text{for } a = 1, 2, 3, \quad (2)$$

$m_a$  being meson masses ( $m_1 = m_\pi$ ,  $m_2 = m_K$  and  $m_3 = m_\eta$ ) and  $s$  is the invariant energy squared. The phase space factor for the four-pion state is defined at  $s < 1 \text{ GeV}^2$  either as two- $\rho$ -meson phase space or as two- $\sigma$ -meson phase space and as unity at  $s > 1 \text{ GeV}^2$ . Thus, for two  $\rho$ -mesons,  $\rho_4(s)$  is expressed by:

$$\rho_4(s) = \begin{cases} \rho_0 \int \frac{ds_1}{\pi} \int \frac{ds_2}{\pi} \frac{M^2 \Gamma(s_1) \Gamma(s_2) \sqrt{(s+s_1-s_2)^2 - 4s s_1}}{s[(M^2-s_1)^2 + M^2 \Gamma^2(s_1)][(M^2-s_2)^2 + M^2 \Gamma^2(s_2)]} & s < 1 \text{ GeV}^2 \\ 1 & s > 1 \text{ GeV}^2 \end{cases} \quad (3)$$

Here  $s_1$  and  $s_2$  are two-pion energies squared,  $M$  is the  $\rho$ -meson mass and  $\Gamma(s)$  is its energy-dependent width:

$$\Gamma(s) = \gamma \rho_1^3(s) \quad (4)$$

The factor  $\rho_0$  provides the continuity of  $\rho_4(s)$  at  $s = 1 \text{ GeV}^2$ . For the  $\sigma\sigma$  intermediate state (the  $\sigma$ -meson is the  $00^{++}$ -state) the phase space factor at  $s < 1 \text{ GeV}^2$  has more cumbersome structure than that of eq.(3); however the results are practically the same as for the  $\rho\rho$  phase space.

For  $K_{ab}$  we use a parametrization similar to that of ref. [17]:

$$K_{ab}(s) = \left( \sum_{\alpha} \frac{g_a^{(\alpha)} g_b^{(\alpha)}}{M_{\alpha}^2 - s} + f_{ab} \frac{1 + s_0}{s + s_0} \right) \frac{s - m_{\pi}^2/2}{s}, \quad (5)$$

where  $g_a^{(\alpha)}$  are coupling constants of the bare state  $\alpha$  to meson channels; parameters  $f_{ab}$  and  $s_0$  describe the smooth part of the K-matrix elements ( $s_0 > 1.5 \text{ GeV}$ ).

Production processes are considered using the technique of initial-state-vector of ref. [18]. Amplitudes of  $\pi\pi$ ,  $K\bar{K}$  and  $\eta\eta$  production in  $\pi N$  collisions due to  $t$ -channel pion exchange can be written as follows:

$$A_{\pi N \rightarrow N a} = g(\bar{\Psi}_N \gamma_5 \Psi_N) F_N(t) D(t) A_{\pi\pi(t) \rightarrow a}, \quad (6)$$

where  $a = \pi\pi$ ,  $K\bar{K}$  or  $\eta\eta$ ;  $F_N(t)$  is the nucleon form factor,  $D(t)$  is the pion propagator (or reggeized pion propagator, for more detail see ref. [17]).  $A_{\pi\pi(t) \rightarrow a}$  is the transition

amplitude which depends on the virtuality of the  $t$ -channel pion. In the initial-state-vector approach, this amplitude is of the form:

$$A_{\pi\pi(t)\rightarrow a} = P_b(1 - i\hat{\rho}\hat{K})_{ba}^{-1}. \quad (7)$$

Here  $\vec{P}$  depends on the virtuality of the initial pion. This vector corresponds to the components of the K-matrix with modified initial-state blocks:

$$P_b = \left( \sum_{\alpha} \frac{\tilde{g}^{(\alpha)}(t)g_b^{(\alpha)}}{M_{\alpha}^2 - s} + \tilde{f}_b(t) \frac{1 + s_0}{s + s_0} \right) \frac{s - m_{\pi}^2/2}{s}. \quad (8)$$

In the limit  $t \rightarrow m_{\pi}^2$ , the expression (7) turns into the scattering amplitude, so:

$$\tilde{g}^{(\alpha)}(t \rightarrow m_{\pi}^2) = g_1^{(\alpha)} \quad \tilde{f}_b(t \rightarrow m_{\pi}^2) = f_{1b}. \quad (9)$$

The part of the amplitudes  $p\bar{p}$  (*at rest*)  $\rightarrow \pi^0\pi^0\pi^0$ ,  $\pi^0\eta\eta$ ,  $\pi^0\pi^0\eta$  which corresponds to the two-meson production in  $00^{++}$  states can be written in the following way [19]:

$$A_{p\bar{p}\rightarrow\text{mesons}} = A_1(s_{23}) + A_2(s_{13}) + A_3(s_{12}). \quad (10)$$

The amplitude  $A_k(s_{ij})$  stands for any interaction of particles in intermediate states but the last interaction is that of particles  $i$  and  $j$  in the state  $00^{++}$ , the particle  $k$  being a spectator. For  $\pi^0\pi^0\pi^0$  production  $A_1 = A_2 = A_3$ , and the amplitude  $A_k$  which describes the final-state interaction of the  $\pi^0\pi^0$  pair in the  $00^{++}$  state is equal to:

$$A_k(s_{ij}) = P_b^{(\pi)}(s_{ij}) \left(1 - i\hat{\rho}\hat{K}\right)_{b1}^{-1}. \quad (11)$$

The components of  $\vec{P}^{(\pi)}$ , where index  $(\pi)$  characterizes the spectator particle, are as follows:

$$P_b^{(\pi)}(s_{ij}) = \left( \sum_{\alpha} \frac{\Lambda_{\alpha}^{(\pi)}g_b^{(\alpha)}}{M_{\alpha}^2 - s_{ij}} + \phi_b^{(\pi)} \frac{1 + s_0}{s_{ij} + s_0} \right) \frac{s_{ij} - m_{\pi}^2/2}{s_{ij}}. \quad (12)$$

Parameters  $\lambda_{\alpha}^{(\pi)}$  and  $\phi_b^{(\pi)}$  may be complex magnitudes with different phases.

The same vector  $\vec{P}^{(\pi)}$  defines the amplitude of the  $00^{++}$   $\eta\eta$ -state in the reaction  $p\bar{p} \rightarrow \pi^0\eta\eta$ :

$$A_1(s_{23}) = P_b^{(\pi)}(s_{23}) \left(1 - i\hat{\rho}\hat{K}\right)_{b3}^{-1}. \quad (13)$$

Production of the  $\pi^0\pi^0$  pair in the reaction  $p\bar{p} \rightarrow \eta\pi^0\pi^0$  is described by eqs. (11) and (12), with the replacement of indices  $(\pi) \rightarrow (\eta)$ . The couplings  $\Lambda_{\alpha}^{(\eta)}$  and  $\phi_b^{(\eta)}$  represent other sets of complex parameters.

**2) Coupling constants in the decays  $f_0 \rightarrow \pi\pi$ ,  $K\bar{K}$ ,  $\eta\eta$ ,  $\eta\eta'$ ,  $\eta'\eta'$  in the quark combinatorics.** In the leading terms of the  $1/N$  expansion, the couplings of  $q\bar{q}$ -mesons and glueball decays to two mesons are determined by the diagrams shown in Figs. 1a, b.

In these processes, gluons produce either one  $q\bar{q}$ -pair ( $q\bar{q}$  decay, Fig. 1a) or two  $q\bar{q}$  pairs (glueball decay, Fig. 1b). The production of soft  $q\bar{q}$  pairs by gluons goes on with the flavour symmetry violation: the direct indication of such a violation comes from multiparticle production in the central hadron collisions at high energies (see ref. [20] and references therein) and from radiative  $J/\Psi$  decays [8]. In these cases the production of strange quarks is suppressed by the same factor  $\lambda$ . The ratios of the production probabilities are:

$$u\bar{u} : d\bar{d} : s\bar{s} = 1 : 1 : \lambda \quad (14)$$

with  $\lambda = 0.4 - 0.5$ . Extending this property to the decays of  $00^{++}$   $q\bar{q}$ -mesons allows us to calculate the ratios of coupling constants  $f_0 \rightarrow \pi\pi, K\bar{K}, \eta\eta, \eta\eta', \eta'\eta'$ . They are given in Table 1 for  $f_0 = n\bar{n} \cos \Phi + s\bar{s} \sin \Phi$ , where  $n\bar{n} = (u\bar{u} + d\bar{d})/\sqrt{2}$ .

In Table 1 we also present the coupling constants taken from ref. [8] for the decay of a glueball. One can see that the glueball decay-couplings satisfy the same relations as  $q\bar{q}$ -meson couplings, with the mixing angle  $\Phi = \Phi_{glueball}$  where

$$\tan \Phi_{glueball} = \sqrt{\frac{\lambda}{2}}. \quad (15)$$

This is the result of the two-stage decay of the glueball (see Fig.1b): the intermediate  $q\bar{q}$ -state in the glueball decay is the mixture of  $n\bar{n}$  and  $s\bar{s}$  quarks with the probabilities given by eq.(14). With  $\lambda = 0.4 - 0.5$ , eq. (15) goes to  $\Phi_{glueball} = 25^\circ \pm 3^\circ$ .

If  $f_0$  is a mixture of the  $q\bar{q}$ -state ( $q\bar{q} = n\bar{n} \cos \phi + s\bar{s} \sin \phi$ ) and the glueball ( $GG$ ),  $f_0 = q\bar{q} \cos \alpha + GG \sin \alpha$ , then coupling constants for the decay of this resonance into two  $q\bar{q}$ -mesons are the same as given in Table 1, with the replacement  $\Phi \rightarrow \Phi_{effective}$ , where

$$\tan \Phi_{effective} = \frac{g\sqrt{2 + \lambda} \sin \Phi + \tilde{g}\sqrt{\lambda} \tan \alpha}{g\sqrt{2 + \lambda} \cos \Phi + \tilde{g}\sqrt{2} \tan \alpha}. \quad (16)$$

The values  $g$  and  $\tilde{g}$  are determined in Table 1.

**3) Fit of the data.** Fitting CERN-Münich data on the reaction  $\pi^- p \rightarrow n\pi^+\pi^-$ , we use the values for moments  $N < Y_L^M >$  provided by this group [3]. The moments with  $M = 0$  and  $M = 1$  are related to the partial amplitudes as follows:

$$\begin{aligned} N < Y_L^0 > &\equiv \sum_{JJ'} \sqrt{\frac{(2J+1)(2J'+1)}{4\pi(2L+1)}} < JJ'00|L0 > \{ < JJ'00|L0 > Re\rho_{00}^{JJ'} \\ &\quad - [1 + (-1)^{J+J'-L}] < JJ'1-1|L0 > Re\rho_{11}^{JJ'} \}, \\ N < Y_L^1 > &\equiv \sum_{JJ'} \sqrt{\frac{(2J+1)(2J'+1)}{4\pi(2L+1)}} < JJ'00|L0 > < JJ'01|L1 > 2Re\rho_{01}^{JJ'} \quad (17) \\ \rho_{00}^{JJ'} &= T_0^J T_0^{J'*}, \quad \rho_{01}^{JJ'} = T_0^J T_-^{J'*}, \quad \rho_{11}^{JJ'} = 2T_-^J T_-^{J'*}, \end{aligned}$$

$$g_0^J = 2C_N \sqrt{\left(\frac{s}{4} - m_\pi^2\right)(2J+1)} A_J(s), \quad g_-^J = \frac{g_0^J}{C_J \sum_{n=0}^3 a_n s^{n/2}}.$$

Here  $J$  and  $J'$  are angular momenta of outgoing pions and  $\langle JJ'mm'|LM\rangle$  are Clebsch-Gordan coefficients. The amplitude  $T_0^J$  describes the  $t$ -channel pion exchange and  $A_J(s)$  is the partial wave amplitude for the transition  $\pi^-\pi^+(t) \rightarrow \pi^-\pi^+$ . The amplitudes with  $J = 0, 1, 2, 3$  and  $I = 0, 1, 2$  have been used in the fit. The data of ref. [3] are selected with small  $t$ -values, in the interval  $t < 0.15$  (GeV/c)<sup>2</sup>. So, when fitting these data, we neglect the  $t$ -dependence in the  $K$ -matrix elements, supposing that it causes only a renormalization of the coefficient  $C_N$ . For the partial wave  $IJ^{PC} = 00^{++}$ , we have used the  $K$ -matrix in the form of eqs. (1)–(9), taking  $\tilde{g}^{(\alpha)}$  and  $\tilde{f}_a$  at  $t = m_\pi^2$ . The treatment of other partial waves is performed in the same way as in ref. [3].

The main contribution into  $T_-^J$  is provided by the  $t$ -channel  $a_1$ -exchange. This amplitude is fitted in the same form as  $T_0^J$  but with additional  $s$ -dependent factor  $C_J \sum a_n s^{n/2}$ , where  $C_J$  and  $a_n$  are free parameters.

The BNL group [5] has performed a partial wave analysis of the experimental data and extracted the amplitude squared  $|A_{\pi\pi(t)\rightarrow K\bar{K}}|^2$ . The events have been selected in a very narrow  $t$ -interval,  $|t| < 0.07$  (GeV/c)<sup>2</sup>; so, as before, we calculate this amplitude at  $t = m_\pi^2$  too.

The  $\pi^-p \rightarrow \pi^0\pi^0n$  events obtained by GAMS [4] are distributed over six  $t$ -intervals (in (GeV/c)<sup>2</sup> units):  $0 < -t < 0.2$ ,  $0.3 < -t < 1$ ,  $0.35 < -t < 1$ ,  $0.4 < -t < 1$ ,  $0.45 < -t < 1$  and  $0.5 < -t < 1$ . The following  $t$ -dependence gives a good description of GAMS data:

$$\tilde{g}^{(\alpha)}(t) = g_1^{(\alpha)} + \left(1 - \frac{t}{m_\pi^2}\right) \frac{t}{m_\pi^2} g'^{(\alpha)}, \quad \tilde{f}_a(t) = f_{1a} + \left(1 - \frac{t}{m_\pi^2}\right) \frac{t}{m_\pi^2} f'_a$$

$$F_N(t) = \left[\frac{\tilde{\Lambda} - m_\pi^2}{\tilde{\Lambda} - t}\right]^4, \quad D(t) = (m_\pi^2 - t)^{-1}. \quad (18)$$

The event number in each  $t$ -interval can be calculated integrating the amplitude squared,  $|A_{\pi N \rightarrow N a}|^2$ , over the corresponding  $t$ -interval.

When fitting Crystal Barrel data [1, 2], we use eqs. (10)–(13) for the  $00^{++}$  wave, while the other partial waves are treated in the same way as described in detail in ref. [1].

**4) Two  $K$ -matrix solutions.** In the simultaneous fit of the data [1–6], we have obtained two groups of  $K$ -matrix solutions. Inside each group, the solutions give similar descriptions of the data; the variations are mainly due to the form used for the  $4\pi$  phase space, or they are related to the parameters which affect the reactions weakly. For example, at the moment we cannot fix in the  $4\pi$  channel the relative probabilities related to two  $\rho$ - and two  $\sigma$ -meson states. Below we discuss two solutions which treat the  $4\pi$  channel in the simplest way ( $\pi\pi\pi\pi = \rho\rho$ ) and keep weakly controlled parameters equal to zero. Parameters for these solutions are given in Table 2.

Both solutions describe well the experimental data: a typical description of the CERN-Münich data is shown in Fig. 2, GAMS data in Fig. 3; the  $\pi\pi \rightarrow K\bar{K}$  and  $\pi\pi \rightarrow \eta\eta$

amplitude squared as well as the  $\pi\pi$  inelastic cross section are drawn in Fig.4. Corresponding  $\chi^2$  values per point are given in the second and fourth columns of Table 3. In our simultaneous fit,  $\chi^2$  for every reaction is not worse than the  $\chi^2$  obtained by various groups in the separate fits of these reactions. For example, in ref. [3] (CERN-Münich data)  $\chi^2$  per point is 2.6 (in our fit  $\chi^2 = 1.8$ ); for  $p\bar{p}$  annihilations  $\chi^2(3\pi^0) = 1.8$ ,  $\chi^2(\pi\eta\eta) = 1.65$  and  $\chi^2(\pi\pi\eta) = 1.6$  [2], while in our fit the corresponding values are about 1.5, 1.5 and 1.4. Relative branching ratio for  $\pi^0\pi^0\pi^0$  and  $\pi^0\eta\eta$  production in  $p\bar{p}$  annihilation is 3.35 for both solutions, which coincides well with the experimental magnitude  $3.1 \pm 0.8$  [2].

The two groups of solutions differ in sign in the K-matrix non-pole term for the transition  $\pi\pi \rightarrow K\bar{K}$  and in the couplings of the first and third K-matrix poles to the  $K\bar{K}$  channel. This affects mainly the description of the  $\pi\pi \rightarrow K\bar{K}$  channel. To improve the second solution for this reaction, the BNL experimental data [5] should be scaled down by a factor 1.20. As is seen from Fig.4a, there is a discrepancy between BNL and Argonne [21] data for this channel, about a factor 1.5, so scaling down the of BNL data by a factor 1.20 could be quite justified. Let us note that such a change of the scale could be also plausible for the first solution, though a lesser effect is required.

All solutions give rather similar positions of singularities of the scattering amplitudes. The positions of the poles on the second and on the third sheets are given in Table 4: they coincide well with the poles obtained in the  $T$ -matrix approach [15]. The other stable characteristics are phase shift and inelasticity in the  $00^{++}\pi\pi$  scattering amplitude. Our results are shown in Fig.5 for the phase shift and in Fig. 6 for the inelasticity.

For the solutions presented in Table 2, the couplings of the K-matrix poles with  $\alpha = 2, 3, 4$  to  $\pi\pi$ ,  $K\bar{K}$  and  $\eta\eta$  channels agree with the quark combinatoric relations given in Table 1, with  $\lambda = 0.45$  and  $\sin\Theta = 0.57$ . Therefore, we have also fitted the data implying for the couplings the constraint given by Table 1. The description of data changed insignificantly;  $\chi^2$  obtained with this constraint is given in the third and fifth columns of Table 3. Relative branching ratios for  $p\bar{p} \rightarrow \pi^0\pi^0\pi^0 / p\bar{p} \rightarrow \pi^0\eta\eta$  are 3.5 for the first solution and 3.6 for the second one. Corresponding parameters (masses of the K-matrix poles,  $\pi\pi$ -channel couplings  $g_1$ ,  $\Phi_{effective}$  and  $4\pi$ -channel couplings  $g_4$ ) are given in Table 5.

Let us emphasize that we do not include in our fit the  $\pi\pi \rightarrow \eta\eta$  data. Nevertheless the two-bump structure of the  $\pi\pi \rightarrow \eta\eta$  amplitude squared is reproduced in both our solutions without  $f_0(1590)$ . This resonance has been seen in the  $\eta\eta'$  spectrum as well [22], hence the incorporation of  $\eta\eta'$  channel into analysis is needed to make a final conclusion about the nature of this resonance; this is beyond our current investigation.

**5) Where is the lowest scalar glueball?** The lightest  $f_0^{bare}$  state has a large  $s\bar{s}$  component: it is approximately the same as in the  $\eta$ -meson. For the states  $f_0^{bare}(1240)$  and  $f_0^{bare}(1615)$  we have not obtained a satisfactory solution with a large  $s\bar{s}$  component. For  $f_0^{bare}(1280)$  the 50%-admixture of the  $s\bar{s}$ -component is permissible; this state may be the  $SU(3)$ -nonet partner for  $f_0^{bare}(750)$ . On the contrary, an assumption that  $f_0^{bare}(1240)$  is the nonet partner of  $f_0^{bare}(750)$  leads to significantly larger  $\chi^2$  value.

For the other two states the following scenarios are possible:

1. There is no glueball among these states, and they are radial excitations of the nonstrange  $q\bar{q}$ -system, while the mixing angles of  $f_0^{bare}$ 's coincide with the glueball angle given by eq.(15) only accidentally. In this case we should expect the existence of two  $s\bar{s}$ -rich  $f_0$  resonances in the region 1550–1850 MeV;
2. One of these states corresponds to the radial excitation of nonstrange quarks and another one is the lowest glueball. For example,  $f_0^{bare}(1240)$  is  $2^1P_0$   $n\bar{n}$ -state, while  $f_0^{bare}(1615)$  is a glueball or vice versa. In both cases only one  $s\bar{s}$ -rich state exists in the region 1550-1850 MeV.

Therefore, the crucial point for the identification of a glueball is to determine the number of  $f_0$  states with large  $s\bar{s}$  component in the mass region 1550–1850 MeV. To fulfill this task a careful analysis of the reactions  $\pi p \rightarrow \eta\eta n$ ,  $\pi p \rightarrow \eta\eta' n$ ,  $p\bar{p} \rightarrow \eta\eta'\pi$ ,  $p\bar{p} \rightarrow K\bar{K}\pi$ , together with the data of refs. [1–6], should be made.

**6) Conclusion.** A K-matrix analysis based on the experimental data of refs. [1–6] has been performed for the wave  $00^{++}$  up to 1550 MeV. Two solutions have been found which determine the positions of K-matrix poles as well as the couplings of these poles with two pseudoscalar mesons and with the  $4\pi$ -channel.

The necessity to use the K-matrix formalism is caused by strong resonance overlapping which is the case for the  $00^{++}$ -wave. It leads to the shift of the poles because of the transitions *resonance*  $\rightarrow$  *real mesons*  $\rightarrow$  *resonance*. To perform a reliable interpretation of  $q\bar{q}$ - or  $GG$ -resonances, the influence of these shifts should be removed. The obtained K-matrix poles,  $f_0^{bare}$ 's, demonstrate that the mass shift due to the transition *resonance*  $\rightarrow$  *real mesons*  $\rightarrow$  *resonance* is rather large, about 100–200 MeV, and actually resonances are strong mixtures of  $f_0^{bare}$ 's and two/four-meson components.

Our analysis shows that coupling constants of the  $f_0^{bare}$  states to the two pseudoscalar-meson channels obey the quark combinatoric rules with good accuracy. These rules argue strongly in favour of one of the bare states,  $f_0^{bare}(1240)$  or  $f_0^{bare}(1615)$ , being considered as a candidate for a glueball. However, for a final conclusion, the investigation of the  $00^{++}$  wave in the region 1550–1850 MeV is needed, especially in the channels strongly coupled to the  $s\bar{s}$  state.

We thank D.V.Bugg, S.S.Gershtein, A.K.Likhoded, L.Montanet, Yu.D.Prokoshkin and B.S.Zou for encouraging discussions and useful remarks. We are grateful to Dr. W. Ochs for supplying CERN-Münich data in numerical form, and also the GAMS and Crystal Barrel groups for making their new high statistics data available. This work was partly supported by the International Science Foundation Grant N 10300.

## References

- [1] V.V. Anisovich et al., Phys. Lett. **B323** (1994) 233;  
C. Amsler et al., Phys. Lett. **B333** (1994) 277.
- [2] C. Amsler et al., Phys. Lett. **B342** (1995) 433.
- [3] B. Hyams et al., Nucl. Phys. **B64** (1973) 134.
- [4] A.A. Kondashov et al., Proc. 27th Intern. Conf. on High Energy Physics, Glasgow (1994) 1407;  
Yu.D. Prokoshkin et al., Physics-Doklady (1995), in press;  
D. Alde et al., "Study of the  $f_0(995)$  resonance in the  $\pi^0\pi^0$  decay channel", Preprint CERN-PPE/94-157, 1994.
- [5] S.J. Lindenbaum and R.S. Longacre, Phys. Lett. **B274** (1992) 492;  
A. Etkin et al., Phys. Rev. **D25** (1982) 1786.
- [6] M. Alston-Garnjost et al., Phys. Lett. **B36** (1971) 152.
- [7] C. Amsler and F.E. Close, Phys. Lett. **B353** (1995) 385;  
S.S. Gershtein, A.K. Likhoded and Yu.D. Prokoshkin, Z. Phys. **C24** (1984) 305.
- [8] V.V. Anisovich, Phys. Lett. **B364** (1995) 195.
- [9] R.L. Jaffe and K. Johnson, Phys. Lett. **B60** (1976) 201;  
J.F. Donoghue, K. Johnson and B.A. Li, Phys. Lett. **B99** (1981) 416.
- [10] J. Paton and N. Isgur, Phys. Rev. **D31** (1985) 2910.
- [11] G.S. Bali et al., Phys. Lett. **B309** (1993) 378;  
R. Gupta et al., Phys. Rev. **D43** (1991) 2301.
- [12] D. Weingarten, Talk at "Gluonium 95", Corsica, 1995;  
H. Chen et al., Nucl. Phys. **B34** (1994) 357.
- [13] G. t'Hooft, Nucl. Phys. **B72** (1974) 461;  
G. Veneziano, Nucl. Phys. **B117** (1976) 519.
- [14] V.V. Anisovich, D.V. Bugg, A.V. Sarantsev and B.S. Zou, Phys. Rev. **D50** (1994) 1972; *ibid* **D50** (1994) 4412.
- [15] D.V. Bugg, A.V. Sarantsev and B.S. Zou, Nucl. Phys. **B**, to be published.
- [16] D. Morgan, "Issues in light hadron spectroscopy", Preprint RAL-93-078 (1993);  
M.R. Pennington, Talk at "Gluonium 95", Corsica, 1995;  
N.A. Törnqvist, Talk at "Gluonium 95", Corsica, 1995.
- [17] V.V. Anisovich et al., Phys. Lett. **B355** (1995) 363.
- [18] I.J.R. Aitchison, Nucl. Phys. **A189** (1972) 417.

- [19] V.V. Anisovich, D.V. Bugg, A.V. Sarantsev and B.S. Zou, Phys. of Atomic Nucl. **57** (1994) 1595.
- [20] V.V. Anisovich, M.G. Huber, M.N. Kobrinsky and B.Ch. Metch, Phys. Rev. **D42** (1990) 3045.
- [21] V.A. Polychronakos et al., Phys. Rev. **D19** (1979) 1317;  
A.D. Martin and E.N. Ozmutlu, Nucl. Phys. **B158** (1979) 520.
- [22] D. Alde et al., Nucl.Phys., **B269** (1986) 485;  
F. Binon et al., Nuovo Cim. **A80** (1984) 363.

## Figure Captions

- Fig. 1.** Diagrams for the decay of (a) a  $q\bar{q}$ -meson and (b) a glueball into two  $q\bar{q}$ -meson states.
- Fig. 2.** Fit of the  $\pi\pi$  angular-moment distributions in the final state of the reaction  $\pi^-p \rightarrow n\pi^+\pi^-$  at 17.2 GeV/c [3]. The curve corresponds to the first K-matrix solution with the resonance decay couplings obeying the quark combinatoric constraints (Table 1).
- Fig. 3.** Event numbers *versus* invariant mass of the  $\pi\pi$ -system for different  $t$ -cuts in the  $\pi^-p \rightarrow \pi^0\pi^0n$  reaction [4]. The solid curve corresponds to the first K-matrix solution with resonance decay couplings obeying the quark combinatoric constraints and the dashed curve to the second one.
- Fig. 4.** a) The  $\pi\pi \rightarrow K\bar{K}$  amplitude squared: data are taken from refs. [5] (circles) and [21] (squares); b) The ratios  $\sigma(\pi\pi \rightarrow 4\pi)/\sigma(\pi\pi \rightarrow \pi\pi)$  [6]; c)  $\pi\pi \rightarrow \eta\eta$  amplitude squared [5]. The style of the curves is the same as in Fig. 3.
- Fig. 5.** The S-wave  $\pi\pi$  phase shift obtained in the simultaneous fit of the data [1–6].
- Fig. 6.** Inelasticity of the  $\pi\pi$  S-wave obtained in the simultaneous fit of the data [1–6].

Table 1

Coupling constants given by quark combinatorics for a  $q\bar{q}$ -meson and glueball decaying into two pseudoscalar mesons;  $\Phi$  is mixing angle for  $n\bar{n}$  and  $s\bar{s}$  states and  $\Theta$  is the mixing angle for  $\eta - \eta'$  mesons:  $\eta = n\bar{n} \cos \Theta - s\bar{s} \sin \Theta$  and  $\eta' = n\bar{n} \sin \Theta + s\bar{s} \cos \Theta$ .

Channel	$q\bar{q}$ -meson decay couplings	Glueball decay couplings
$\pi^0\pi^0$	$g_\pi \equiv g \cos \Phi / \sqrt{2}$	$G_\pi \equiv \tilde{g} / \sqrt{2 + \lambda}$
$\pi^+\pi^-$	$g_\pi$	$G_\pi$
$K^+K^-$	$g_\pi(\sqrt{2} \tan \Phi + \sqrt{\lambda})/2$	$G_\pi\sqrt{\lambda}$
$K^0K^0$	$g_\pi(\sqrt{2} \tan \Phi + \sqrt{\lambda})/2$	$G_\pi\sqrt{\lambda}$
$\eta\eta$	$g_\pi (\cos^2 \Theta + \sqrt{2\lambda} \tan \Phi \sin^2 \Theta)$	$G_\pi (\cos^2 \Theta + \lambda \sin^2 \Theta)$
$\eta\eta'$	$g_\pi \sin \Theta \cos \Theta (1 - \sqrt{2\lambda} \tan \Phi)$	$G_\pi \cos \Theta \sin \Theta (1 - \lambda)$
$\eta'\eta'$	$g_\pi (\sin^2 \Theta + \sqrt{2\lambda} \tan \Phi \cos^2 \Theta)$	$G_\pi (\sin^2 \Theta + \lambda \cos^2 \Theta)$

Table 2

Parameters (in GeV units) for the K-matrix solutions without quark combinatoric constraints on the coupling constants  $g_n^{(\alpha)}$ .

	I solution				II solution			
	$\alpha = 1$	$\alpha = 2$	$\alpha = 3$	$\alpha = 4$	$\alpha = 1$	$\alpha = 2$	$\alpha = 3$	$\alpha = 4$
M	0.651	1.235	1.269	1.565	0.858	1.209	1.281	1.583
$g_1^{(\alpha)}$	1.012	0.800	0.185	0.484	0.694	0.961	0.241	0.547
$g_2^{(\alpha)}$	-0.774	0.495	0.063	0.050	0.029	0.551	0.246	0.146
$g_3^{(\alpha)}$	0.073	0.228	0.045	0.155	-0.081	0.232	0.053	0.167
$g_4^{(\alpha)}$	0	0	0.537	0.383	0	0	0.556	0.455
$Re(\Lambda_\alpha^{(\pi)})$	-0.193	-0.013	2.036	1	-0.186	-0.100	1.832	1
$Im(\Lambda_\alpha^{(\pi)})$	-0.621	-0.641	-0.389	0	-0.509	-0.654	-0.014	0
$Re(\Lambda_\alpha^{(\eta)})$	1	0.084	-0.770	0	1	-0.348	-2.484	0
$Im(\Lambda_\alpha^{(\eta)})$	0	0.241	0.145	0	0	-1.023	-3.112	0
$g'_\alpha$	0.024	-0.048	0	0	0.022	-0.046	0	0
	a=1	a=2	a=3	a=4	a=1	a=2	a=3	a=4
$f_{1a}$	0.398	-0.607	0	0	0.034	0.286	0	0.050
$Re(\phi_a^{(\pi)})$	-0.661	0.434	0.139	0	-0.551	-0.465	0.194	0
$Im(\phi_a^{(\pi)})$	-0.559	0.413	0.074	0	-1.102	-0.841	-0.040	0
$Re(\phi_a^{(\eta)})$	1.461	-0.643	0	0	2.742	2.719	0	0
$Im(\phi_a^{(\eta)})$	1.191	-0.943	0	0	4.756	2.311	0	0
$f'_a$	0.076	-0.030	0	0	0.089	-0.074	0	0
	$s_0 = 1.8$		$\tilde{\Lambda} = 0.149$		$s_0 = 5.0$		$\tilde{\Lambda} = 0.154$	

Table 3

The  $\chi^2$  values for the K-matrix solutions without and with quark combinatoric constraint.

	I solution		II solution	
	without quark combinatoric constraint	with $g_n^{(\alpha)}$ given by Table 1	without quark combinatoric constraint	with $g_n^{(\alpha)}$ given by Table 1
$p\bar{p} \rightarrow \pi^0\pi^0\pi^0$	1.50	1.53	1.52	1.57
$p\bar{p} \rightarrow \pi^0\eta\eta$	1.50	1.50	1.54	1.53
$p\bar{p} \rightarrow \pi^0\pi^0\eta$	1.34	1.34	1.39	1.42
$\pi^+\pi^- \rightarrow \pi^+\pi^-$	1.75	1.81	1.72	1.78
$\pi^+\pi^- \rightarrow \pi^0\pi^0$	1.87	1.97	1.92	2.08
$\pi\pi \rightarrow K\bar{K}$	0.68	0.54	0.88	0.51
$\pi\pi \rightarrow 4\pi$	3.60	3.50	3.53	3.07

Table 4

Pole positions (in MeV) in the  $00^{++}$  partial wave amplitude (2nd sheet: under  $\pi\pi$  and  $4\pi$  cuts; 3rd sheet: under  $\pi\pi$ ,  $4\pi$  and  $K\bar{K}$  cuts; 4th sheet: under  $\pi\pi$ ,  $4\pi$ ,  $K\bar{K}$  and  $\eta\eta$  cuts).

I solution			II solution		
2nd sheet	3rd sheet	4th sheet	2nd sheet	3rd sheet	4th sheet
1015 - i46	936 - i238	1280 - i116 1311 - i512 1501 - i64	1004 - i41	957 - i41	1285 - i128 1490 - i613 1498 - i64

Table 5

Masses, coupling constants (in GeV) and mixing angles of the  $f_0^{bare}$ -resonances.

	I solution				II solution			
	$\alpha = 1$	$\alpha = 2$	$\alpha = 3$	$\alpha = 4$	$\alpha = 1$	$\alpha = 2$	$\alpha = 3$	$\alpha = 4$
M	0.651	1.254	1.280	1.601	0.805	1.242	1.265	1.632
$\Delta M$	+0.200 -0.020	+0.010 -0.035	$\pm 0.025$	+0.050 -0.025	+0.030 -0.160	$\pm 0.025$	+0.025 -0.015	+0.025 -0.050
$g_1^{(\alpha)}$	0.869	0.798	0.261	0.607	0.563	0.958	0.414	0.751
$\Delta g_1^{(\alpha)}$	+0.200 -0.250	$\pm 0.050$	+0.060 -0.100	+0.150 -0.060	+0.130 -0.030	+0.030 -0.110	+0.030 -0.100	+0.020 -0.200
$g_4^{(\alpha)}$	0	0	0.774	0.494	0	0	0.624	0.627
$\Delta g_4^{(\alpha)}$	0	0	+0.020 -0.200	+0.150 -0.050	0	0	+0.150 -0.150	+0.050 -0.150
$\Phi_\alpha(deg)$	-58 <sup>+20</sup> <sub>-5</sub>	17 <sup>+10</sup> <sub>-15</sub>	14 <sup>+15</sup> <sub>-30</sub>	-10 <sup>+25</sup> <sub>-20</sub>	-36 <sup>+15</sup> <sub>-25</sub>	13 $\pm$ 15	16 $\pm$ 30	-5 <sup>+30</sup> <sub>-10</sub>
	$25^\circ > \Phi_3 - \Phi_2 > 0^\circ$				$25^\circ > \Phi_3 - \Phi_2 > 0^\circ$			

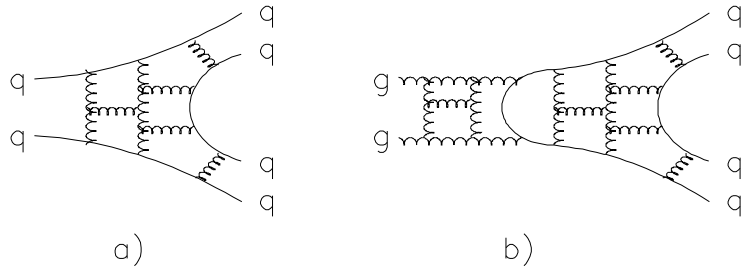


Fig.1

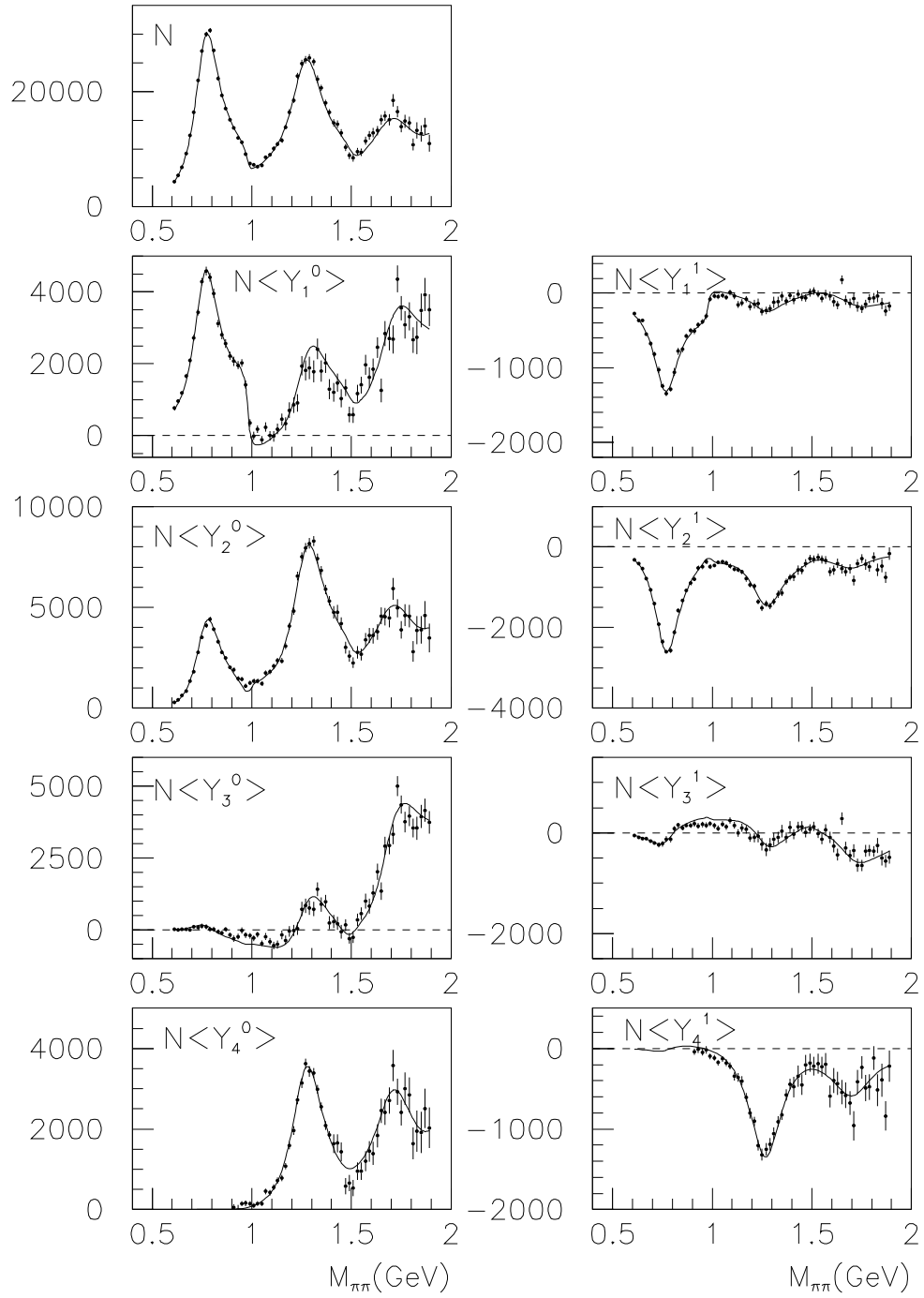


Fig.2

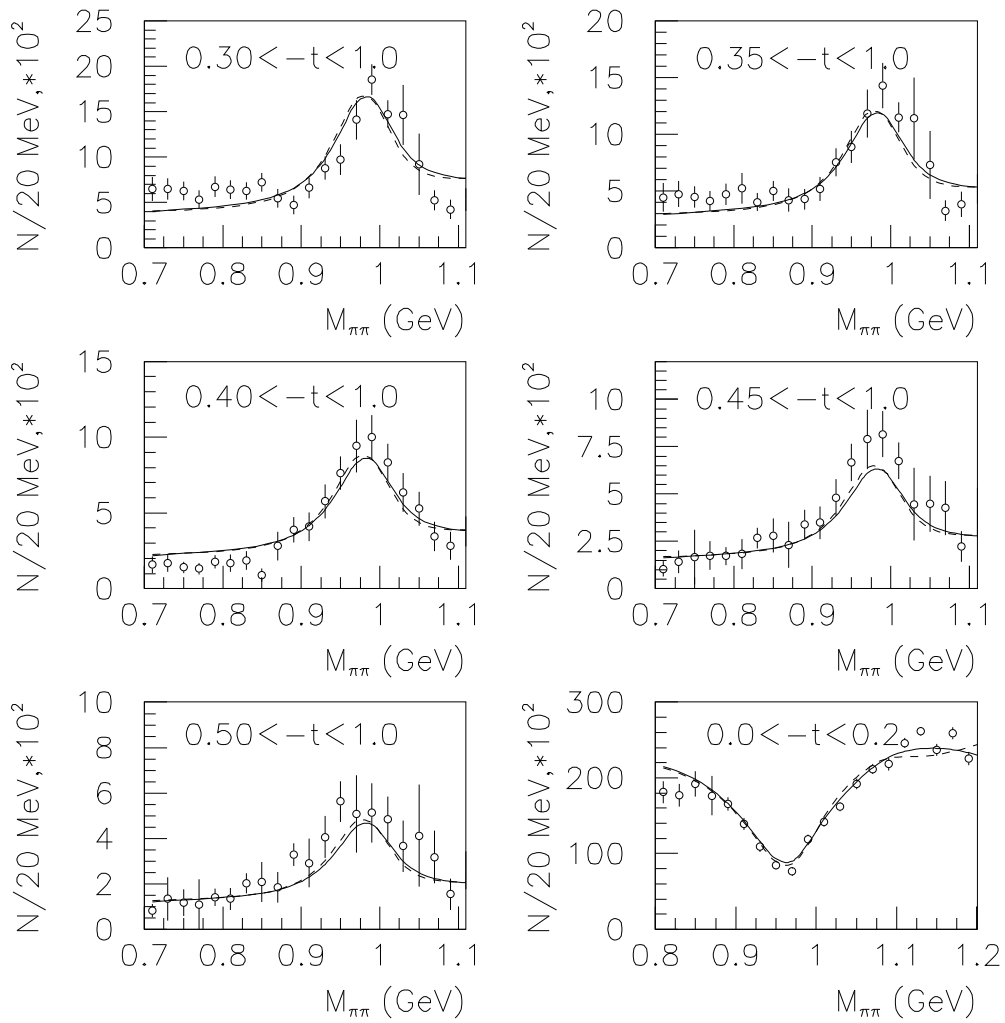


Fig.3

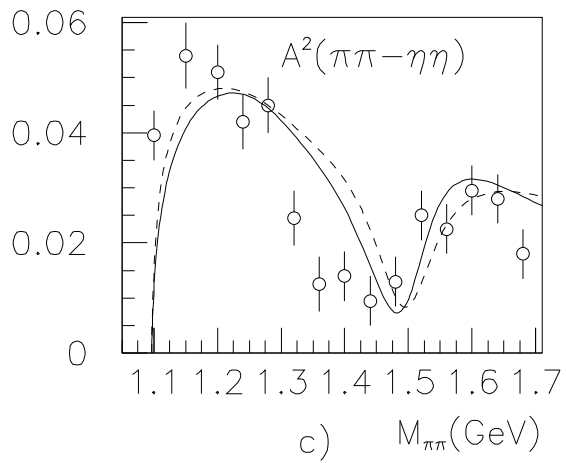
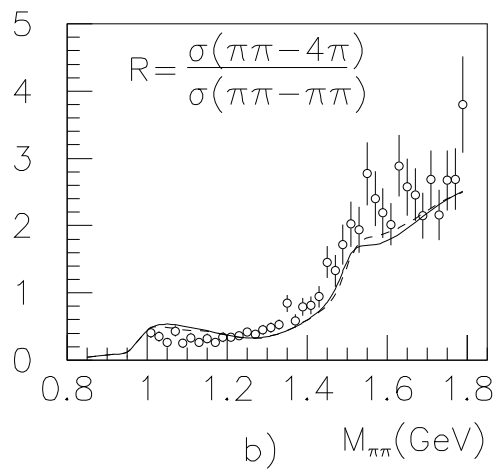
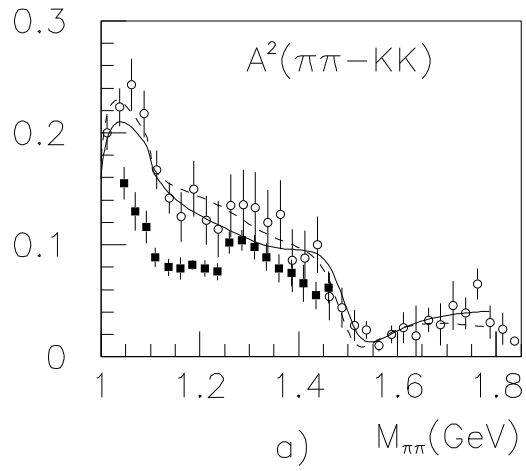


Fig.4

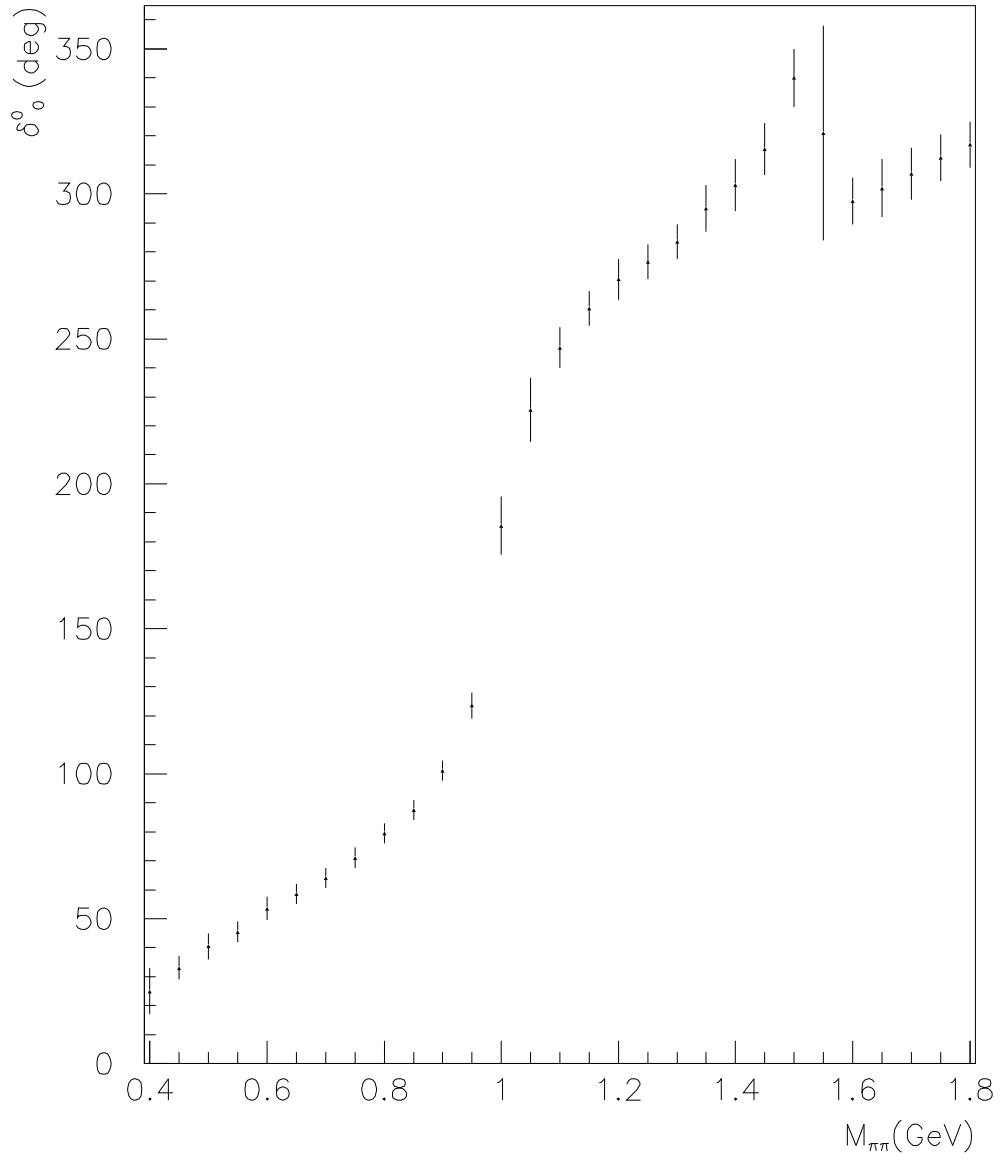


Fig.5

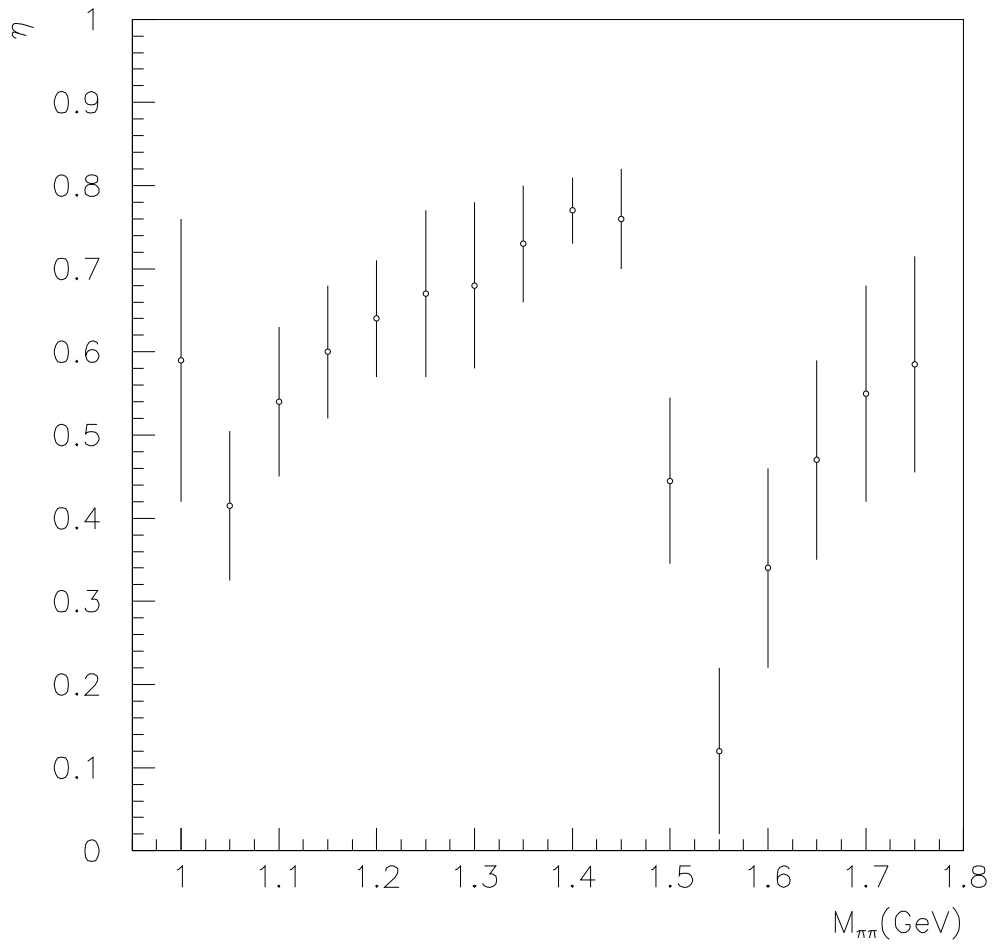


Fig.6